



Tomographic Inversion of the 135.6 nm Emission: The Importance of Radiation Transport in the Nighttime and Terminator Regions

Kenneth Dymond, Andrew Nicholas, Scott Budzien, Andrew Stephan,
& Clayton Coker

Naval Research Laboratory

Keith Groves
Boston College

This work was sponsored by the Chief
of Naval Research through NRL 6.1
base funding.

Introduction (1 of 2)

- Previous work at NRL and in a recent paper published in the *JGR* emphasized the importance of radiation transport when modeling/interpreting the 135.6 nm nightglow
 - JGR paper discusses tomographic solution (Qin, J., et al. (2015), *J. Geophys. Res. Space Physics*, 120, 10116–10135, doi:10.1002/2015JA021687.)
 - NRL work used 1D inversion code (Dymond, K. F., et al. (1997) *Radio Science*, Vol. 32, No. 5, 1985-1996).
 - Both studies used *plane parallel* radiation transport in the Complete Frequency Redistribution approximation
 - Additionally, both studies showed the importance of modeling and including the Mutual Neutralization source of the 135.6 nm emission

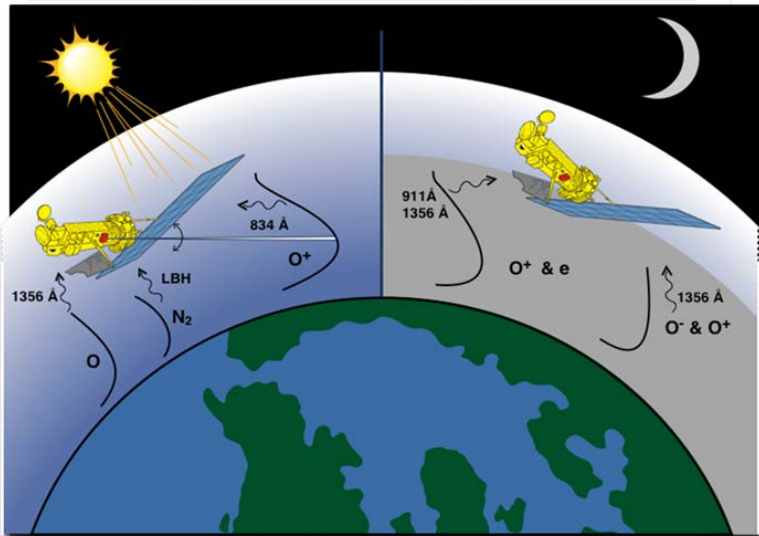
Introduction (2 of 2)

- What are we trying to learn?
 - How important is the modeling of the Mutual Neutralization source when calculating the electron densities in practical cases?
 - How important is the inclusion of Radiation Transport in practical cases?
 - If proper modeling of these two sources of emission is included, is it possible to interpret 135.6 nm emission measurements in the region of the solar terminator?
 - Is 2D radiation transport required in the terminator region?
- We used coincident measurements of the latitude-altitude distribution of electrons using the incoherent scatter radar at ALTAIR during overflights of the SSULI sensor in the DMSP satellites to answer these questions

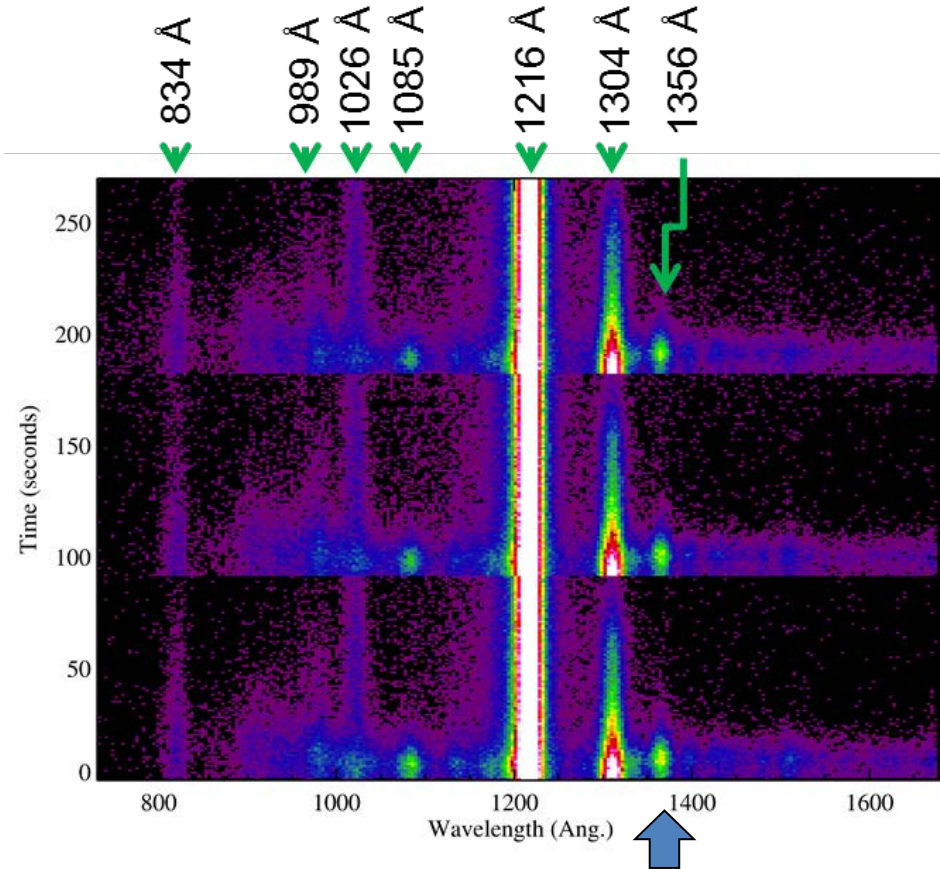
SSULI Measurement Scenario



SSULI Processing Algorithm and Data Products		
Solar Zenith Angle	Algorithm	EDR Data Products
SA < 85°	Dayside Ionosphere Algorithm (Requires 834 SDRs)	O ⁺ Density Profile, hmF2, nmF2
SA >= 108°	Nightside Ionosphere Algorithm (Requires 1356 and 911 SDRs)	O ⁺ , O Density Profiles, hmF2, nmF2
SA < 85°	Dayside Neutral Density Algorithm (Requires 1356 and LBH SDRs)	O, N ₂ , O ₂ Density Profiles, Temperature Profile.



3 Daytime Limb Scans



135.6 nm, Focus of this talk

O I 135.6 nm: Photon Production

- The 135.6 nm emission is excited by three sources:
 - Radiative recombination:
 - $O^+ + e^- \rightarrow O + h\nu$ (135.6 nm)
 - Mutual Neutralization:
 - $O^+ + O^- \rightarrow O + O^*(^5S) \rightarrow 2O(^3P) + h\nu$ (135.6 nm)
 - Photoelectron Impact:
 - $O + e^- \rightarrow O^*(^5S) + e^- \rightarrow O(^3P) + h\nu$ (135.6 nm) + e^-

- In the dayglow, the 135.6 nm is contaminated by an underlying emission from the photoelectron impact excited N_2 in the Lyman-Birge-Hopfield band at 135.3 nm
 - $N_2 + e^- \rightarrow N_2^* + e^- \rightarrow N_2 + h\nu$ (LBH bands) + e^-

O I 135.6 nm : Nighttime Chemistry Model

- At night the two sources of 135.6 nm emission are Radiative Recombination and Mutual Neutralization
- The equation below is used to calculate the electron density from the volume emission rate using Newton-Raphson iteration
 - Initial guess for electron density estimated assuming first term is zero
 - NRLMSISE-00 used to estimate O density
 - Coefficients taken from: Meléndez-Alvira, et al. (1999), *J. Geophys. Res.*, 104(A7), 14901–14913, doi:10.1029/1999JA900136.

$$\varepsilon_0(z) = \gamma \underbrace{\beta_{1356} \frac{k_1 k_2 n_e(z) n_o(z) n_{o^+}(z)}{k_2 n_{o^+}(z) + k_3 n_o(z)}}_{\text{Mutual Neutralization}} + \gamma \underbrace{\alpha_{1356} n_e(z) n_{o^+}(z)}_{\text{Radiative Recombination}}$$

O I 135.6 nm : Radiation Transport

- The 1356 Å emission is a doublet and is scattered by atomic oxygen and absorbed by molecular oxygen:
 - O: Resonant Scattering redistributes the photons in altitude
 - $O + h\nu (135.6, 135.8 \text{ nm}) \rightarrow O + h\nu (135.6, 135.8 \text{ nm})$, Cross-section: $\sigma = 2.499 \times 10^{-18} \text{ cm}^2 (135.6)$; $\sigma = 1.242 \times 10^{-18} \text{ cm}^2 (135.8)$
 - O₂: Absorption removes photons
 - $O_2 + h\nu (135.6, 135.8 \text{ nm}) \rightarrow 2O$, Cross-section: $\sigma = 7.20 \times 10^{-18} \text{ cm}^2 (135.6)$; $\sigma = 7.15 \times 10^{-18} \text{ cm}^2 (135.8)$
- Integral version of the radiation transport equation in the plane-parallel Complete Frequency Redistribution approximation:

$$\varepsilon(z) = \varepsilon_0(z) + n_o(z) \sigma \int_{z_{\min}}^{z_{\max}} \varepsilon(z') H(|\tau(z) - \tau(z')|, |t(z) - t(z')|) dz' \quad \left\{ \begin{array}{l} \tau(z) = \sigma \int_z^{\infty} n_o(z') dz' \\ t(z) = \sigma_{O_2}^{abs} \int_z^{\infty} n_{O_2}(z') dz' \end{array} \right.$$

$$\text{Holstein H function} \rightarrow H(\tau, t) = \frac{1}{2\sqrt{\pi}} \int e^{-2x^2} E_1(\tau e^{-x^2} + t) dx$$

O I 135.6 nm: Radiation Transfer

- Once the photons are created and then scattered or redistributed in altitude, one needs to model the transfer of that radiation to the observer for observation:

$$I_{1356} = 10^{-6} \sum \int_0^{\infty} T(|\tau(z(s)) - \tau^s(z(s=0))|, |t^s(z(s)) - t^s(z(s=0))|) \varepsilon(z(s)) ds$$

- The function, T , is the Holstein t-function:
 - x is the width of the spectral line in Doppler units

$$T(\tau, t) = \frac{1}{\sqrt{\pi}} \int_{-\infty}^{\infty} e^{-x^2} \exp(-\tau e^{-x^2} + t) dx$$

$$4\pi I = 10^{-6} \sum \varepsilon(s(z, \lambda, \phi)) T(|\tau(s_i) - \tau(s=0)|, |t(s_i) - t(s=0)|) \Delta s_i$$

System of equations solved using VERT approach

O I 135.6 nm : Volume Emission Rate Tomography (VERT)

$$4\pi I = 10^{-6} \sum \varepsilon(s(z, \lambda, \phi)) T(|\tau(s_i) - \tau(s=0)|, |t(s_i) - t(s=0)|) \Delta s_i$$

- Iteratively solve the intensity system of equations (above) to infer the volume emission rate
 - Non-negative solution based on Richardson-Lucy algorithm
 - Seeks log-likelihood solution based on Poisson statistics
- Approach uses a physicality constraint applied between iterations
 - Regularization to the isotropic diffusion equation
 - This method outperforms Maximum A Posteriori (MAP) and Tikhonov regularization approaches
- Very rapid convergence

$$\mathbf{x}^{[k+1]} \simeq \frac{\mathbf{x}^{[k]}}{\mathbf{A}^T(\mathbf{1})} \otimes \mathbf{A}^T \left(\frac{\mathbf{b}}{\mathbf{A}\mathbf{x}^{[k]}} \right)$$

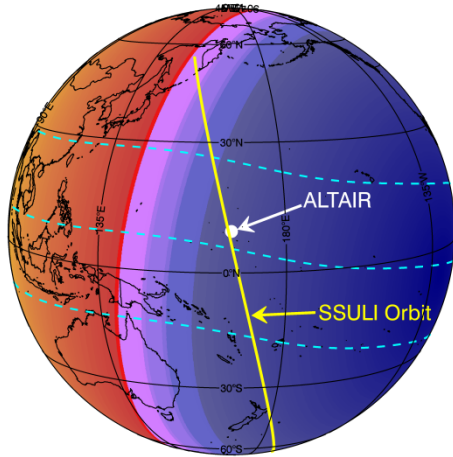
Division and multiplication are elementwise

Inversion Approach

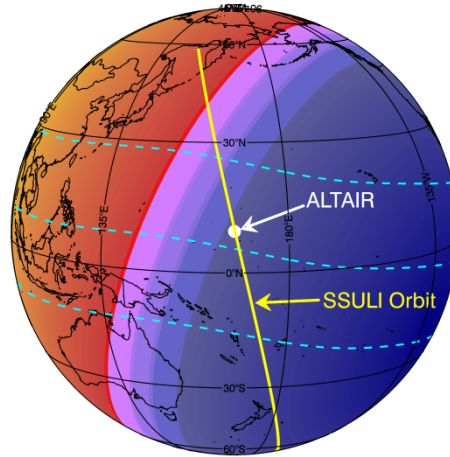
- Use SSULI 135.6 nm measurements made over ALTAIR during 2010 (DMSP-F18) and 2014 (DMSP-F19)
 - 2010 measurements made at ~20 LT → nighttime
 - 2014 measurements made at ~1820 LT → nighttime/terminator
- Use Volume Emission Rate Tomography (VERT) to produce the 2D distribution of photon emission (volume emission rate) in the orbit plane
 - Account for Radiation Transfer due to resonant scattering and pure absorption in the path-length matrices used in VERT
 - Use NRLMSISE-00 model to estimate the O and O₂ densities
- Use inverse CFR Radiation Transport to remove the resonant scattering contribution to the volume emission rate
- Solve the Nighttime Chemistry Model to determine the electron density
- Compare electron density to ALTAIR measurements

DMSP F18 Observations

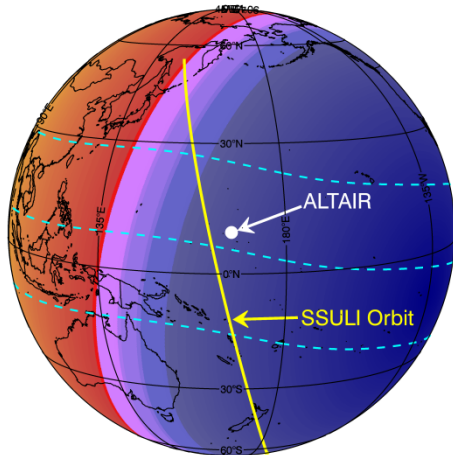
6 April 2010



25 July 2010



26 August 2010



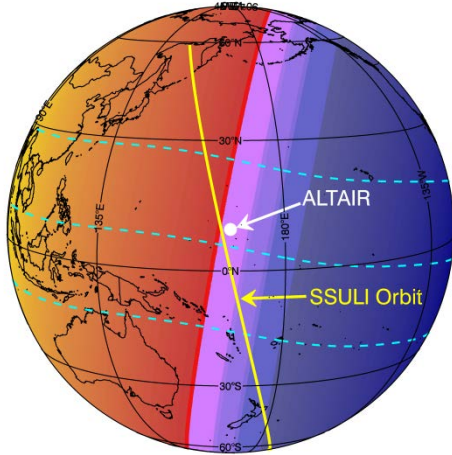
All observations made
when the
solar zenith angle (ζ):
 $\zeta > 105^\circ$

F18 ALTAIR Over-flights

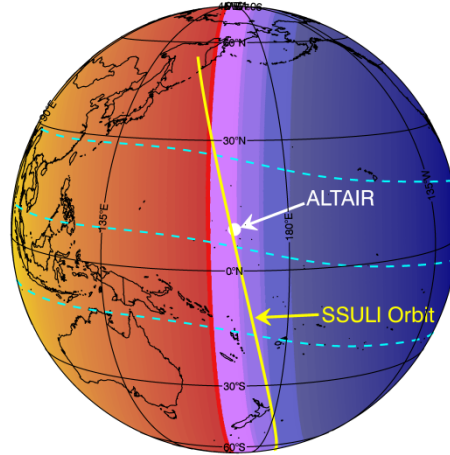
Date	UT (Hr: Min)	Local Time (Hrs)
April 6	08:40	19.9
July 16	08:46	20.0
July 17	08:34	20.0
July 24	08:53	19.9
July 25	08:41	19.9
August 1	08:58	20.0
August 2	08:46	19.9
August 11	08:40	19.9
August 19	08:45	20.0
August 26	09:02	20.0
August 27	08:50	20.0

DMSP F19 Observations

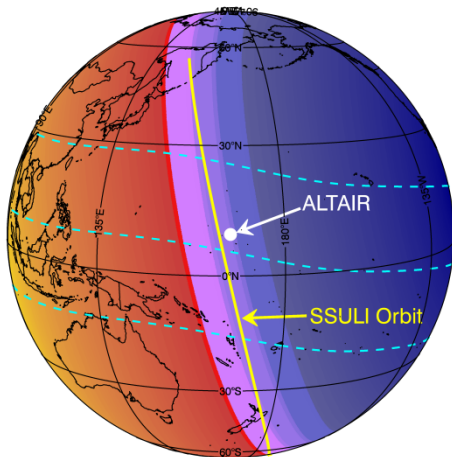
27 August 2014



27 September 2014



27 October 2014



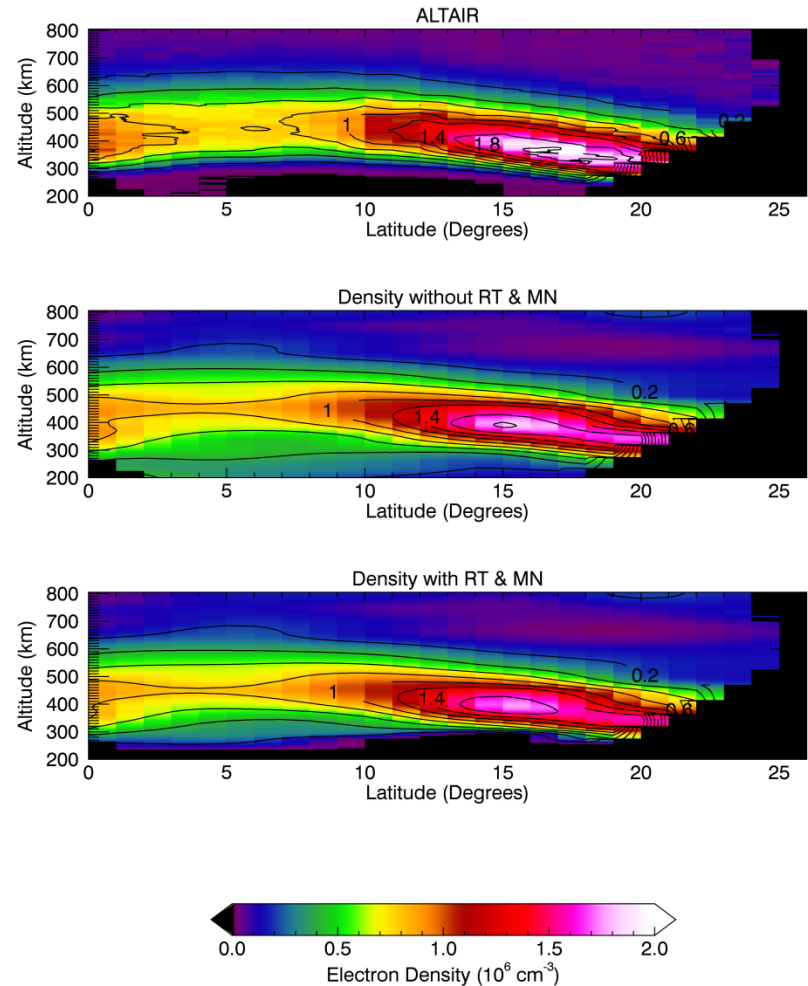
All observations made
when the
solar zenith angle (ζ):
 $90^\circ < \zeta < 100^\circ$

F19 ALTAIR Over-flights

Date	UT (Hr: Min)	Local Time (Hrs)
August 19	07:13	18.4
August 27	07:09	18.3
September 3	07:04	18.2
September 11	07:13	18.4
September 19	07:08	18.3
September 27	07:04	18.2
October 12	07:08	18.3
October 27	07:12	18.4

Typical F18 Inversion & Comparison

- Electron Density Maps: 4/6/2010
 - Top: ALTAIR Density
 - Middle: SSULI Inversion, NO RT & MN
 - Bottom: SSULI Inversion, with RT & MN
- Including Radiation Transport and Radiation Transfer modifies the bottomside, where O scattering dominates
- Mean difference between SSULI and ALTAIR:
 - 27% without MN & RT
 - 15% with MN & RT

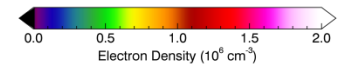
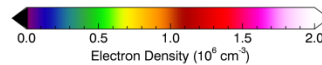
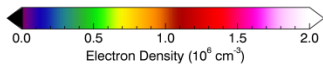
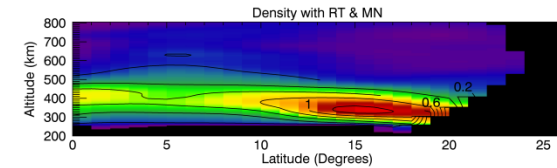
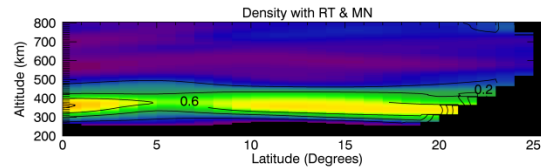
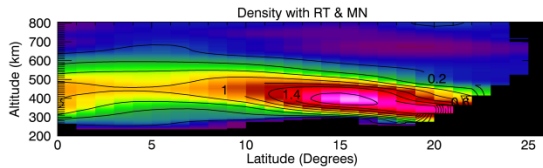
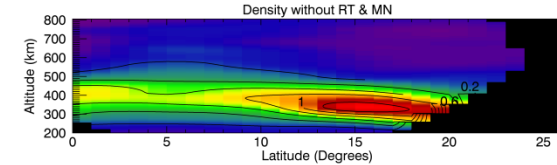
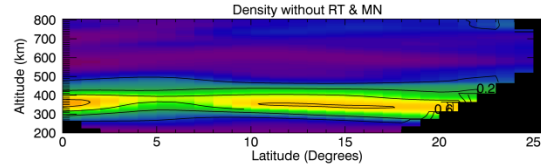
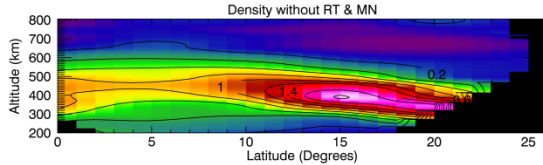
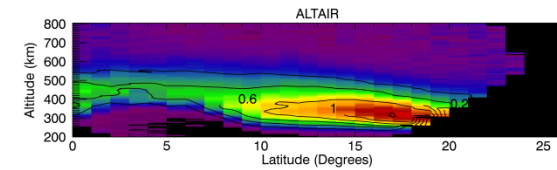
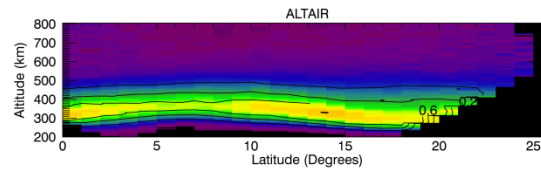
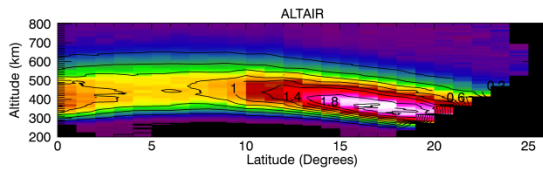


F18 Comparison: Representative Time Series

6 April 2010

25 July 2010

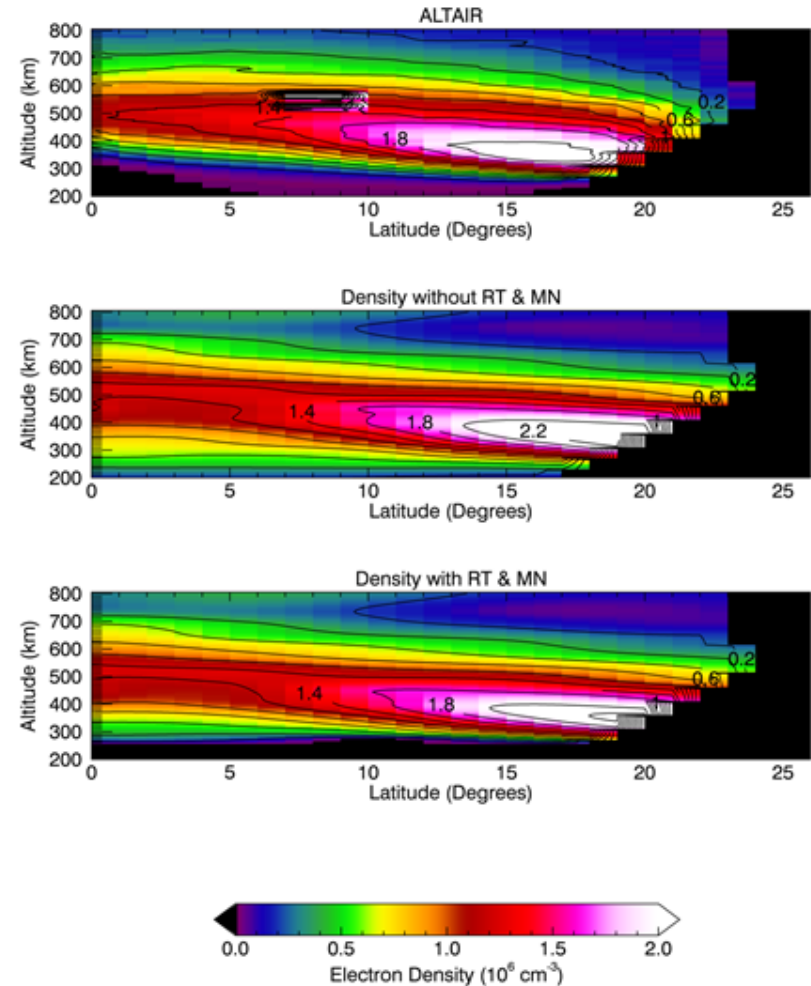
26 August 2010



- SSULI inversions agreed well with ALTAIR even for weak ionospheres
 - Peak densities were often $\sim 5 \times 10^5 \text{ cm}^{-3}$
 - Due to solar minimum conditions

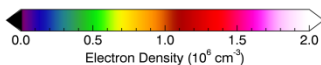
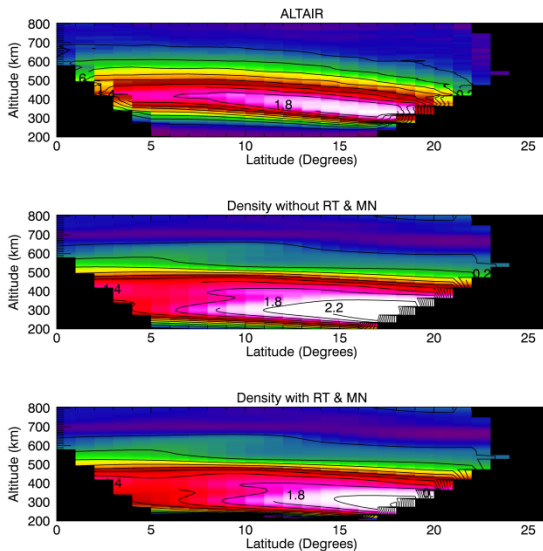
Typical F19 Inversion & Comparison

- Electron Density Maps: 9/27/2014
 - Top: ALTAIR Density
 - Middle: SSULI Inversion, NO RT & MN
 - Bottom: SSULI Inversion, with RT & MN
- Including Radiation Transport and Radiation Transfer modifies the bottomside, where O scattering dominates
- Mean difference between SSULI and ALTAIR:
 - 7% without MN & RT
 - 1% with MN & RT

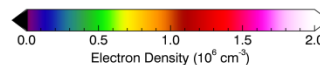
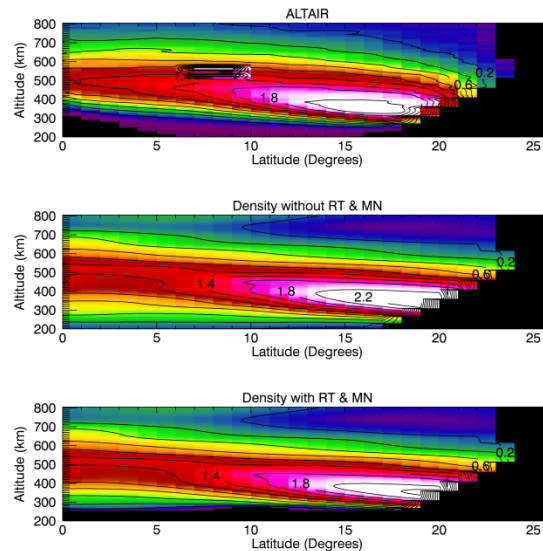


F19 Comparison: Representative Time Series

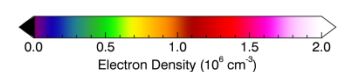
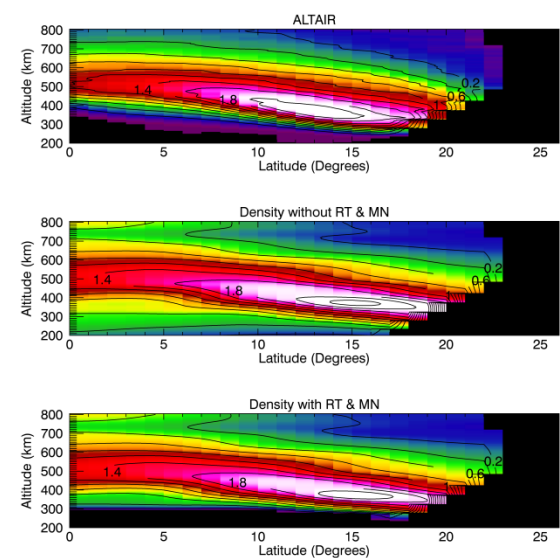
27 August 2014



27 September 2014



27 October 2014

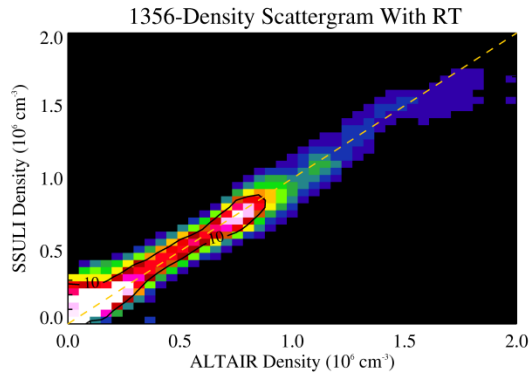


- Agreement between SSULI inversions and ALTAIR improves as the solar zenith angle during the observations increases
 - The leakage of the dayglow into the bottomside is largest during August and decreases through September and October
 - Note that peak densities often exceed $\sim 2 \times 10^6 \text{ cm}^{-3}$, due to solar maximum conditions

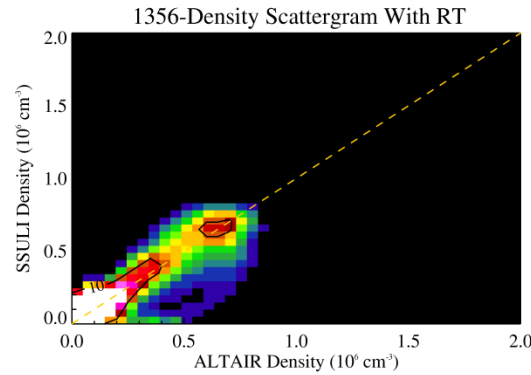
Correlation Comparison

SSULI F18

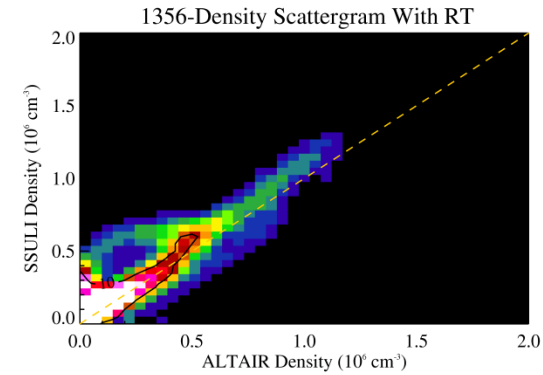
6 April 2010



25 July 2010

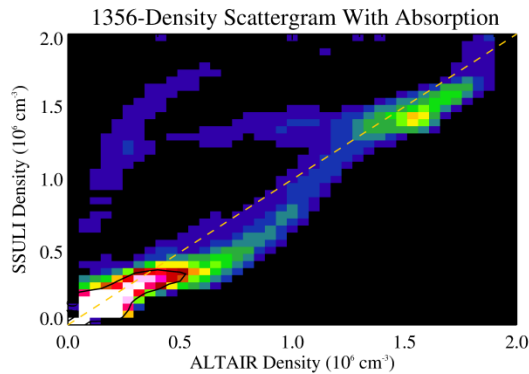


26 August 2010

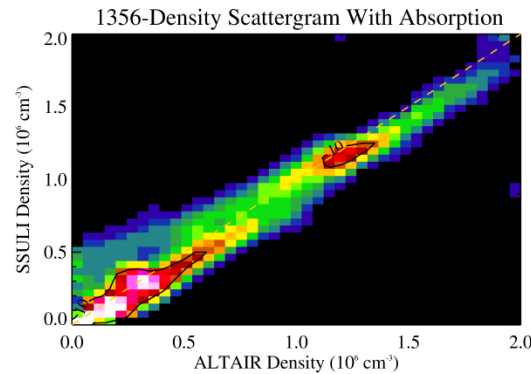


SSULI F19

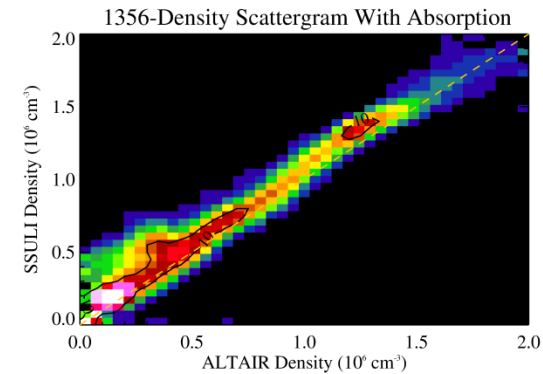
27 August 2014



27 September 2014



27 October 2014



Summary of SSULI Retrievals Against ALTAIR

SSULI F18

Date	Mean Fractional Difference	
	No RT & MN	With RT & MN
2010-04-06	0.272	0.148
2010-07-16	0.232	0.111
2010-07-17	0.197	0.085
2010-07-24	0.063	-0.045
2010-07-25	0.070	-0.045
2010-08-01	0.079	-0.095
2010-08-02	0.160	0.023
2010-08-11	0.251	0.090
2010-08-19	0.115	-0.051
2010-08-26	0.433	0.320
2010-08-27	0.362	0.170
Overall	0.203	0.065

SSULI F19

Date	Mean Fractional Difference	
	No RT & MN	With RT & MN
2014-08-19	0.731	0.595
2014-08-27	0.332	0.220
2014-09-04	0.382	0.278
2014-09-11	0.141	0.067
2014-09-19	0.283	0.169
2014-09-27	0.068	-0.011
2014-10-12	-0.006	-0.108
2010-10-27	0.224	0.142
Overall	0.233	0.052

↑
Nighttime
↓

- *Mean fractional differences are shown*
- *Retrievals including Radiation Transport and Mutual Neutralization generally perform better*

Summary

- We compared electron densities inferred using SSULI 135.6 nm UV tomography to ALTAIR
 - The F18 nighttime measurements were used to validate the technique
 - The F19 measurements were made in the terminator region, which are typically not used because they are difficult to interpret
 - Excellent agreement with the altitude/latitude distributions from the two measurements for the nighttime passes
 - Some dayglow contamination seen in the F19 measurements from 2014
- Our analysis approach entailed
 - Iterative VERT Algorithm -- Richardson-Lucy technique -- handles Poisson noise explicitly and is non-negative
 - Physicality constraint using regularization to the isotropic diffusion equation
 - Inclusion of Mutual Neutralization, Radiative Transfer, and Radiative Transport provided the best results
- Our results indicate the 2D Radiation Transport is likely not needed in the terminator region, however additional research is needed to be able to use the terminator data for ionospheric specification

Acknowledgements

- The SSULI program and part of this research was supported by USAF/Space and Missile Systems Center (SMC).
- The Chief of Naval Research also supported this work through the Naval Research Laboratory (NRL) 6.1 Base Program.

- Introduction (2)
- SSULI Measurement Scenario
- O I 135.6 nm Emission Physics
 - Photon Production
 - Nighttime Chemistry Model
 - Radiation Transport
 - Radiation Transfer
 - Volume Emission Rate Tomography (VERT)
- Inversion Approach
- Observations
 - DMSP F18
 - DMSP F19
- Inversions & Comparison to ALTAIR
 - Typical F18 Inversion & Comparison: August 27?, 2010
 - F18 Time Series
 - Typical F19 Inversion & Comparison: August 27, 2014
 - F19 Time Series
 - Correlation Comparison
- Summary